Aalborg University
ISSN 1395-7953 R0301

Comparing a $k-\varepsilon$ Model and the v^2-f Model in a 3D Isothermal Wall Jet

Lars Davidson*
Dept. of Thermo and Fluid Dynamics
Chalmers University of Technology
SE-412 96 Göteborg, Sweden
http://www.tfd.chalmers.se/~lada

Peter V. Nielsen
Dept. of Building Technology and Structural Engineering
Aalborg University
Sohngaardsholmsvej 57
DK-9000 Aalborg, Denmark
http://www.civil.auc.dk/i6/staff/navn/i6pvn.html

1 Abstract

In this work the flows in a three-dimensional wall jet and in a fully developed plane channel are computed. Two different turbulence models are used, the low-Re $k-\varepsilon$ model of Abe *et al.* (1994) and the $\overline{v^2}-f$ model of Durbin (1991). Two modifications of the $\overline{v^2}-f$ model are proposed. In the original model the wall-normal stress $\overline{v^2}$ is allowed to exceed $2k/3$, although it is supposed to be the smallest of the normal stresses. A simple modification of the $\overline{v^2}-f$ model is proposed which takes care of this problem.
In the $\overline{v^2}-f$ model, two velocity scales are available, $k^{1/2}$ and $(\overline{v^2})^{1/2}$, where the latter is the wall-normal fluctuations which are dampened by the wall. In the second modification of the $\overline{v^2}-f$ model we propose to use two viscosities, one ($\nu_{t,\perp}$) – based on $(\overline{v^2})^{1/2}$ – for the turbulent diffusion in the wall-normal direction, and the other ($\nu_{t,\parallel}$) – based on $k^{1/2}$ – for the turbulent diffusion in the wall-parallel directions.

*Part of this work was carried out during the first author's stay at Dept. of Building Technology and Structural Engineering, Aalborg University in Autumn 2002.

2 Introduction

In rooms ventilated with mixed ventilation the flow is usually supplied through an inlet device mounted on a wall just below the ceiling. The resulting flow is a wall jet developing along the ceiling. The flow in this wall jet determines the flow in the whole room. Thus it is very important to be able to predict the flow in the wall jet in order to be able to design the ventilation system.

The flow in an isothermal three-dimensional wall jet is the subject of the present work. It is well known that the spreading rates of a wall jet are very different in the wall-normal and the spanwise directions. The reason for the behavior is the presence of the wall which inhibits the turbulence in the wall-normal direction and hence also the spreading. According to the measurement by Abrahamsson *et al.* (1997), the spreading rates in the wall-normal and spanwise direction are $dy_{1/2}/dx = 0.065$ and $dz_{1/2}/dx = 0.32$, respectively. The large spreading rate in the spanwise direction is created by a strong secondary motion, generated by the normal stresses (Craft & Launder, 2001), analogous to how secondary motion in a square duct is generated. Whereas the magnitude of secondary motion in a square duct is approximately one percent of the streamwise velocity (Pallares & Davidson, 2000), the secondary motion in a three-dimensional wall jet is much larger. Abrahamsson *et al.* (1997) report values of up to 18% (scaled with the local streamwise velocity), and predictions employing second-moment closures of Craft & Launder (2001) show spanwise velocities of up to almost 0.3.

In the present study we use a low-Re $k-\varepsilon$ model (Abe *et al.*, 1994) and the $\overline{v^2}-f$ model (Durbin, 1991). Two modifications are proposed for the $\overline{v^2}-f$ model.

1. In the $\overline{v^2}-f$ model, a transport equation is solved for the wall-normal stress $\overline{v^2}$. The idea is to model the reduction of $\overline{v^2}$ as walls are approached. Thus $\overline{v^2}$ should be smaller than the other normal stresses, which means that $\overline{v^2} \leq 2k/3$ since $k = (\overline{u^2}+\overline{v^2}+\overline{w^2})/2$. This relation is not satisfied in the standard $\overline{v^2}-f$ model. In the present work a simple modification is proposed which gives $\overline{v^2} \leq 2k/3$ everywhere. The modification is shown to work well in fully developed channel flow and for the 3D wall jet.

2. In the $\overline{v^2}-f$ model, two turbulent velocity scales are available, $(\overline{v^2})^{1/2}$ and $k^{1/2}$. In eddy-viscosity models – including the $\overline{v^2}-f$ model – the turbulent diffusion is modelled employing an isotropic turbulent viscosity using one turbulent velocity scale and one turbulent length-scale. Since in the $\overline{v^2}-f$ model we have two turbulent velocity scales, the $\overline{v^2}-f$ model is in the present work modified so that one turbulent viscosity ($\nu_{t,\perp}$) – computed with $(\overline{v^2})^{1/2}$ – is used for the turbulent

Mesh	$\Delta x_{min},\ \Delta x_{max}$	$\Delta y_{min},\ \Delta y_{max}$	$\Delta z_{min},\ \Delta z_{max}$	$(N_y, N_z)_{in}$
1	$5.4 \cdot 10^{-4},\ 0.14$	$1.6 \cdot 10^{-4}, 0.045$	$4.3 \cdot 10^{-4},\ 0.015$	$21, 9$
2	$1.62 \cdot 10^{-3},\ 0.07$	$1.7 \cdot 10^{-4}, 0.039$	$2.1 \cdot 10^{-4},\ 0.027$	$31, 15$

Table 1: Details of the meshes. Number of grid points (N_x, N_y, N_z) *for Mesh 1 & 2 are* $(82, 92, 76)$ *and* $(112, 116, 82)$*, respectively. Maximum stretching for Mesh 1 is* $(f_x, f_y, f_z) = (1.1, 1.1, 1.07)$ *and for Mesh 2* $(f_x, f_y, f_z) = (1.05, 1.08, 1.06)$*. In the table are given minimum and maximum cells size in each direction and number of cells that cover the inlet,* $(N_y \times N_z)_{in}$*.*

diffusion in the wall-normal direction, and another one ($\nu_{t,\|}$) – computed with $k^{1/2}$ – is used for the turbulent diffusion in the wall-parallel directions.

The report is organized as follows. First a short description of the numerical method is presented. In the following section, the turbulence models and the proposed modifications are described. Then the results are presented and discussed, and in the final section some conclusions are drawn.

3 Numerical Method

The finite volume computer program CALC-BFC (**B**oundary **F**itted **C**oordinates) for three-dimensional flow (Davidson & Farhanieh, 1995) is used in this study. The program uses collocated grid arrangement, Cartesian velocity components, and the pressure-velocity coupling

The convective terms in the momentum equations are discretized using the second-order, bounded scheme of van Leer (1974). The convective terms in the equations for turbulent quantities are discretized with hybrid upwind/central differencing (Patankar, 1980).

4 Turbulence Models

4.1 The AKN Model

The low-Re $k-\varepsilon$ model of Abe *et al.* (1994) reads

$$\begin{aligned} \frac{\partial \bar{U}_j k}{\partial x_j} &= \frac{\partial}{\partial x_j}\left[\left(\nu + \frac{\nu_t}{\sigma_k}\right)\frac{\partial k}{\partial x_j}\right] + P_k - \varepsilon \\ \frac{\partial \bar{U}_j \varepsilon}{\partial x_j} &= \frac{\partial}{\partial x_j}\left[\left(\nu + \frac{\nu_t}{\sigma_\varepsilon}\right)\frac{\partial \varepsilon}{\partial x_j}\right] + C_{\varepsilon 1}\frac{\varepsilon}{k}\left(P_k - C_{\varepsilon 2} f_2 \frac{\varepsilon^2}{k}\right) \end{aligned} \tag{1}$$

$$
\begin{aligned}
\nu_t &= C_\mu^k f_\mu \frac{k^2}{\varepsilon} \\
f_\mu &= \left[1 - \exp\left(-\frac{y^*}{14}\right)\right]\left[1 + \frac{5}{R_t^{3/4}} \exp\left\{-\left(\frac{R_t}{200}\right)^2\right\}\right] \\
f_2 &= \left[1 - \exp\left(-\frac{y^*}{3.1}\right)\right]\left[1 - 0.3 \exp\left\{-\left(\frac{R_t}{6.5}\right)^2\right\}\right] \\
y^* &= \frac{u_\varepsilon y}{\nu},\ u_\varepsilon = (\varepsilon\nu)^{1/4}
\end{aligned}
\tag{2}
$$

Boundary conditions for ε at walls is

$$
\varepsilon = \frac{2\nu k}{y^2} \tag{3}
$$

The coefficients are

C_μ^k	$C_{\varepsilon 1}$	$C_{\varepsilon 2}$	σ_k	σ_ε
0.09	1.5	1.9	1.4	1.4

4.2 The $\overline{v^2} - f$ Model

In the $v^2 - f$ model of Durbin (1991, 1993, 1996) two additional equations are solved: the wall-normal stress $\overline{v^2}$ and a function f. This is a model which is aimed at improving modelling of the effects of walls on the turbulence. Walls affect the fluctuations in the wall-normal direction $\overline{v^2}$ in two ways.

1. The wall damping of $\overline{v^2}$ is felt by the turbulence fairly far from the wall ($y^+ \lesssim 200$) through the pressure field;

2. Viscous damping takes place within the viscous and buffer layer ($y^+ \lesssim 20$).

In usual eddy-viscosity models both these effects are accounted for through damping functions. The damping of $\overline{v^2}$ is in the Reynolds stress models accounted for through the modelled pressure-strain terms $\Phi'_{22,1}$ and $\Phi'_{22,2}$.

In the $v^2 - f$ model the problem of accounting for the wall damping of $\overline{v^2}$ is simply resolved by solving the transport equation of $\overline{v^2}$. The $\overline{v^2}$ equation in boundary-layer form reads (Davidson, 2002)

$$
\frac{\partial \rho \bar{U} \overline{v^2}}{\partial x} + \frac{\partial \rho \bar{V} \overline{v^2}}{\partial y} = \frac{\partial}{\partial y}\left[(\mu + \mu_t)\frac{\partial \overline{v^2}}{\partial y}\right] - 2\overline{v \partial p / \partial y} - \rho \varepsilon_{22} \tag{4}
$$

in which the diffusion term has been modelled with an eddy-viscosity assumption (Davidson, 1995, 2002). Note that the production term $P_{22} = 0$

because in boundary-layer approximation $\bar{V} \ll \bar{U}$ and $\partial/\partial x \ll \partial/\partial y$. A model for the dissipation ε_{22} is taken as

$$\varepsilon_{22}^{model} = \frac{\overline{v^2}}{k}\varepsilon$$

Adding ε_{22}^{model} on both sides of Eq. 4 yields

$$\begin{aligned} \frac{\partial \rho \bar{U} \overline{v^2}}{\partial x} + \frac{\partial \rho \bar{V} \overline{v^2}}{\partial y} + \rho \frac{\overline{v^2}}{k}\varepsilon = \\ \frac{\partial}{\partial y}\left[(\mu + \mu_t)\frac{\partial \overline{v^2}}{\partial y}\right] - 2\overline{v\partial p/\partial y} - \rho\varepsilon_{22} + \rho\frac{\overline{v^2}}{k}\varepsilon \end{aligned} \tag{5}$$

A new variable $\mathcal{P}$ is now defined as

$$\mathcal{P} = -\frac{2}{\rho}\overline{v\partial p/\partial y} - \varepsilon_{22} + \frac{\overline{v^2}}{k}\varepsilon \tag{6}$$

so that Eq. 5 can be written as

$$\frac{\partial \rho \bar{U} \overline{v^2}}{\partial x} + \frac{\partial \rho \bar{V} \overline{v^2}}{\partial y} = \frac{\partial}{\partial y}\left[(\mu + \mu_t)\frac{\partial \overline{v^2}}{\partial y}\right] + \rho\mathcal{P} - \rho\frac{\overline{v^2}}{k}\varepsilon \tag{7}$$

$\mathcal{P}$ is the source term in the $\overline{v^2}$-equation above, and it includes pressure-strain and the difference between modelled and exact dissipation. Physically, the main agent for generating wall-normal stress is indeed the pressure-strain term (Davidson, 2002).

When $y \to 0$ we find from Eq. 6 that

$$\mathcal{P} = \mathcal{O}(y^2) \tag{8}$$

A new variable $f = \mathcal{P}/k$ is defined and a relaxation equation is formulated for f as

$$\begin{aligned} L^2\frac{\partial^2 f}{\partial y^2} - f &= -\frac{\Pi_{22}}{k} - \frac{1}{T}\left(\frac{\overline{v^2}}{k} - 2/3\right) \\ T &= \max\left\{\frac{k}{\varepsilon}, C_T\left(\frac{\nu}{\varepsilon}\right)\right\} \\ \frac{\Pi_{22}}{k} &= \frac{C_1}{T}\left(\frac{2}{3} - \frac{\overline{v^2}}{k}\right) + C_2\frac{\nu_t}{k}\left(\frac{\partial \bar{U}}{\partial y}\right)^2 \\ L &= C_L \max\left\{\frac{k^{3/2}}{\varepsilon}, C_\eta\left(\frac{\nu^3}{\varepsilon}\right)^{1/4}\right\} \end{aligned} \tag{9}$$

where Π_{22} is the model of Launder *et al.* (1975), the first term being the slow term, and the second the rapid term.

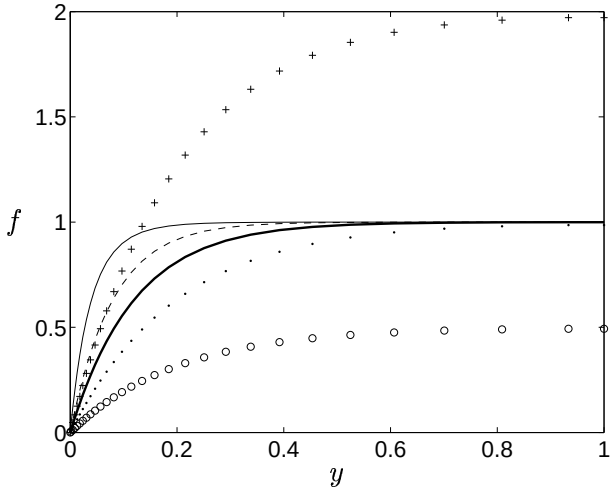

Figure 1: Equation 12 with different L and S. Thin solid line: $L = 0.04, S = 1$; dashed line: $L = 0.08, S = 1$; thick solid line: $L = 0.12, S = 1$; dots: $L = 0.2, S = 1$; +: $L = 0.2, S = 2$; ∘: $L = 0.2, S = 0.5$.

From Eq. 9 we get that $f = \mathcal{O}(y^0)$ as $y \to 0$, and thus the near-wall behavior of $\mathcal{P}$ is enforced. Far from the wall when $\partial^2 f/\partial y^2 \simeq 0$, Eq. 9 yields

$$kf \equiv \mathcal{P} \to \Pi_{22} + \varepsilon(\overline{v^2}/k - 2/3) \tag{10}$$

When this expression is inserted in Eq. 7 we get

$$\frac{\partial \rho \bar{U} \overline{v^2}}{\partial x} + \frac{\partial \rho \bar{V} \overline{v^2}}{\partial y} = \frac{\partial}{\partial y}\left[(\mu + \mu_t)\frac{\partial \overline{v^2}}{\partial y}\right] + \rho \Pi_{22} - \frac{2}{3}\rho\varepsilon \tag{11}$$

which is the usual form of the modelled $\overline{v^2}$-equation with isotropic dissipation. Thus the f equation acts so as to let f go from its wall value to the value of its source term over scale L. In this way the reduction of $\mathcal{P}$ in Eq. 7 as the wall is approached is modelled. The behavior of the equation for f (Eq. 9) for different right-hand sides is illustrated in Fig. 1 where the equation

$$L^2 \frac{\partial^2 f}{\partial y^2} - f + S = 0 \tag{12}$$

has been solved for different L and S. As can be seen f approaches the value of the source term as $y > L$.

4.3 The $\overline{v^2} - f$ model of Lien & Kalitzin (2001)

Lien & Kalitzin (2001) proposed a modification of the $v^2 - f$ model allowing the simple explicit boundary condition $f = 0$ at walls. This modified model

is used in the present work. The $\overline{v^2}$ and f-equation read (Lien & Kalitzin, 2001)

$$\frac{\partial \bar{U}_j \overline{v^2}}{\partial x_j} = \frac{\partial}{\partial x_j}\left[(\nu + \nu_t)\frac{\partial \overline{v^2}}{\partial x_j}\right] + kf - 6\frac{\overline{v^2}}{k}\varepsilon \tag{13}$$

$$L^2 \frac{\partial^2 f}{\partial x_j \partial x_j} - f - \underbrace{\frac{1}{T}\left[(C_1 - 6)\frac{\overline{v^2}}{k} - \frac{2}{3}(C_1 - 1)\right]}_{Term\ 1} \underbrace{+C_2 \frac{P_k}{k}}_{Term\ 2} = 0$$

$$P_k = \nu_t \left(\frac{\partial \bar{U}_i}{\partial x_j} + \frac{\partial \bar{U}_j}{\partial x_i}\right)\frac{\partial \bar{U}_i}{\partial x_j} \tag{14}$$

$$T = \max\left\{\frac{k}{\varepsilon}, 6\left(\frac{\nu}{\varepsilon}\right)^{1/2}\right\}$$

$$L = C_L \max\left\{\frac{k^{3/2}}{\varepsilon}, C_\eta \left(\frac{\nu^3}{\varepsilon}\right)^{1/4}\right\}$$

The turbulent viscosity is computed from

$$\nu_t = C_\mu \overline{v^2} T \tag{15}$$

The k and ε-equations are also solved (without damping functions). Boundary conditions at the walls are

$$k = \overline{v^2} = f = 0,\ \varepsilon = 2\nu k / y^2 \tag{16}$$

The coefficients are given the following values:

C_μ	$C_{\varepsilon 2}$	σ_k	σ_ε	C_1	C_2	C_L	C_η
0.22	1.9	1	1.3	1.4	0.3	0.23	70

and $C_{\varepsilon 1} = 1.4(1 + 0.05(k/\overline{v^2})^{1/2})$.

Note that in the $\overline{v^2}$–f model $\overline{v^2}$ denotes a generic wall-normal fluctuation component rather than the fluctuation in the y direction. This is achieved by the source – kf which is the modelled pressure-strain term – which is affected by the closest wall.

4.3.1 Modification I

The source term kf in the $\overline{v^2}$-equation (Eq. 13) is the modeled pressure strain term which is dampened near walls as f goes to zero. Since $\overline{v^2}$ represents the wall-normal normal stress, it should be the smallest normal stress, i.e. $\overline{v^2} \leq \overline{u^2}$ and $\overline{v^2} \leq \overline{w^2}$, and thus $\overline{v^2}$ should be smaller than $\frac{2}{3}k$ since $k = (\overline{u^2} + \overline{v^2} + \overline{w^2})/2$. In the homogeneous region far away from the wall, the

Laplace term is assumed to be negligible i.e. $\partial^2 f/\partial x_j \partial x_j \to 0$. Then Eq. 14 reduces to (cf. Eq. 10)

$$f_{hom} = -\frac{1}{T}\left[(C_1 - 6)\frac{\overline{v^2}}{k} - \frac{2}{3}(C_1 - 1)\right] + C_2\frac{P_k}{k} \tag{17}$$

It turns out that in the region far away from the wall, the Laplace term is not negligible, and as a consequence $\overline{v^2}$ gets too large so that $\overline{v^2} > \frac{2}{3}k$. A simple modification is to set an upper bound on the source term kf in the $\overline{v^2}$-equation as

$$\overline{v^2}_{source} = \min\left\{kf, -\frac{1}{T}\left[(C_1 - 6)\overline{v^2} - \frac{2k}{3}(C_1 - 1)\right] + C_2 P_k\right\} \tag{18}$$

This modification ensures that $\overline{v^2} \leq 2k/3$. In regions where $\overline{v^2} \simeq 2k/3$, the turbulent viscosity with the $\overline{v^2} - f$ model is $2 \cdot 0.22k^2/(3\varepsilon) = 0.147k^2/\varepsilon$ (see Eq. 15) which is considerably larger than the standard value in the $k - \varepsilon$ model, $0.09k^2/\varepsilon$. A simple remedy is to compute ν_t as

$$\nu_t = \min\left\{0.09k^2/\varepsilon, 0.22\overline{v^2}T\right\} \tag{19}$$

Equations 18 and 19 are called "Modification I", unless otherwise stated.

4.3.2 Modification II

In the $v^2 - f$ model we have two velocity time scales, $(\overline{v^2})^{1/2}$ and $k^{1/2}$. The wall-normal stress $\overline{v^2}$ is dampened near walls as f goes to zero. Thus it is natural to introduce two viscosities, one for wall-normal diffusion ($\nu_{t,\perp}$) and one for diffusion parallel to the wall ($\nu_{t,\|}$) In the present study, we propose to compute them as

$$\nu_{t,\perp} = 0.22\overline{v^2}T, \quad \nu_{t,\|} = 0.09kT \tag{20}$$

For a wall parallel to the $x - z$ plane (at $y = 0$, for example), the turbulent diffusion terms are computed as

$$\begin{array}{c} \dfrac{\partial}{\partial y}\left(\nu_{t,\perp}\dfrac{\partial \Phi}{\partial y}\right) \\ \dfrac{\partial}{\partial x_j}\left(\nu_{t,\|}\dfrac{\partial \Phi}{\partial x_j}\right), j \neq 2 \end{array} \tag{21}$$

where Φ denotes a velocity component. Equation 21 could also be used for the turbulent quantities, but the effect is largest in the momentum equations, and in the present work Eq. 21 is used only in the momentum equations.

5 Results

5.1 Channel Flow

In Fig. 2 channel flow predictions are presented. The computations are carried out as 1D simulations, and the Reynolds number based on the friction velocity is $Re_\tau = u_*\delta/\nu = 590$, where δ denotes half-width of the channel. The number of cells used to cover half of the channel is 64, and a geometric stretching factor of 1.08 is used. The node adjacent to the wall is located at $y^+ = 0.14$. The results presented in Fig. 2 have been obtained using the $\overline{v^2} - f$ model.

From 2a it can be seen that the velocity profile is only very little affected by Modification I. The $\overline{v^2}$ profile is much better predicted with Modification I, as can be seen from Fig. 2b. Without the modification, $\overline{v^2}$ becomes too large for $y^+ > 150$, and it is also seen from Fig. 2c that $\overline{v^2}$ for $y^+ > 400$ erroneously becomes larger than $2k/3$.

In Fig. 2d it can be seen that Modification I reduces f. The reason is that we have a positive feedback: the modification reduces $\overline{v^2}$ by reducing its source (Eq. 18), which in turn reduces f by reducing part of its source $(6 - C_1)\overline{v^2}/k$, which further reduces the source in the $\overline{v^2}$ equation and so on.

The turbulent viscosity is presented in Fig. 2e using either Eq. 15 or Eq. 19. It can be seen that switching from the $\overline{v^2} - f$ expression (Eq. 15) to the $k - \varepsilon$ expression has only a small effect on the computed ν_t. For $y^+ > 380$ the viscosity from the $k - \varepsilon$ expression becomes larger than ν_t from the $\overline{v^2} - f$ model. The effects this switching have on the results in Fig. 2a-d are negligible.

In Fig. 2f the source terms in the f equation are depicted. It can be seen that near the wall Term 2 is largest, and that is because the velocity $\partial\bar{U}/\partial y$ in the P_k is largest here. Furthermore, it is seen that, overall, the largest contribution is given by $-f$. The sum of the source terms – which nowhere goes to zero – is balanced by $(1/L^2)\partial^2 f/\partial y^2$.

5.2 The Wall Jet

The configuration is shown in Fig. 3. The square inlet is located at the uppermost part of the left wall and the outlet (a slot) is situated at the lowermost part of the right wall. Since the geometry is symmetric only half of the configuration is considered.

In Fig. 4 the y^+ values for the nodes adjacent to the walls are depicted. Along the upper wall, y^+ is mostly below one (for $x/H > 0.5$), and the largest values are found along the vertical right wall for which y^+ reaches values of approximately 12.

In Figs. 5 - 10 predicted half widths (defined as the position where $\bar{U}(x, y, z)$ is half of $\bar{U}_{max}(x)$), horizontal and vertical velocity profiles, $\bar{U}$ contours and ν_t contours are presented using the AKN model on mesh 1 & 2

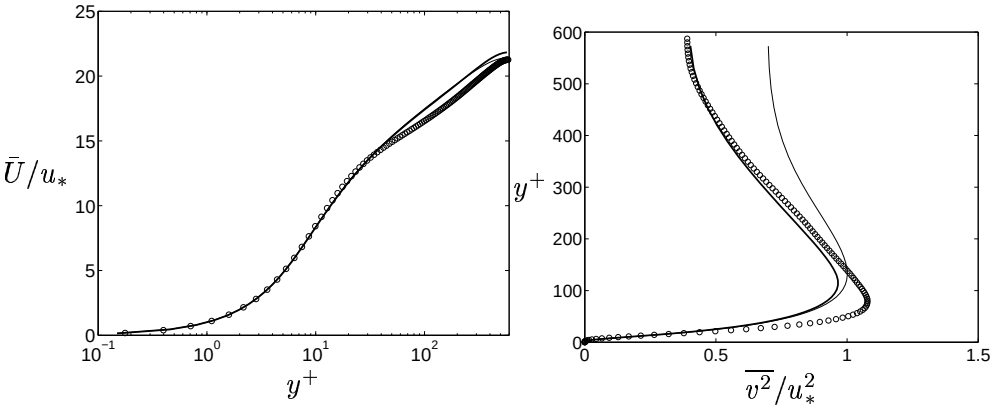

(a) $\bar{U}$-velocity.

(b) Wall-normal stress..

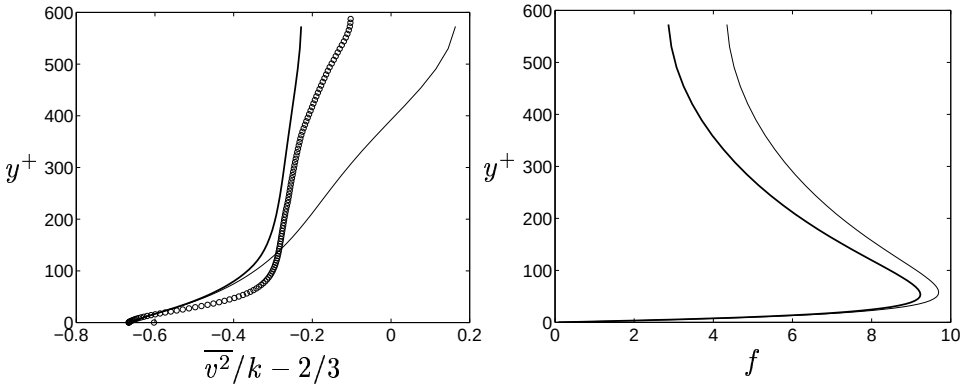

(c) Wall-normal anisotropy.

(d) f-function.

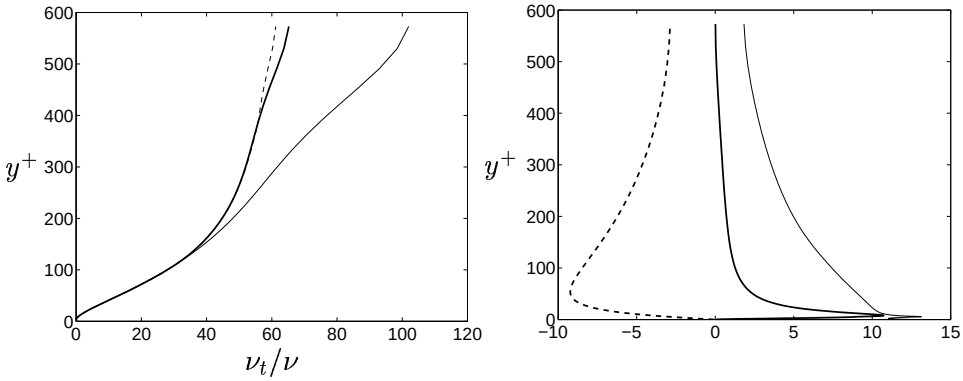

(e) Thick solid line line: Modification I, ν_t from Eq. 15; dashed line: Modification I and ν_t from Eq. 19.

(f) Source terms in f equation, Eq. 14. Modification I. Thin solid line: Term 1; thick solid line: Term 2; f: thick dashed line.

Figure 2: Channel flow. $Re_\tau = 590$. $\overline{v^2} - f$ model. Thin solid line: standard model; thick solid lines: Modification I. Circles represent DNS of Moser et al. *(1999)*

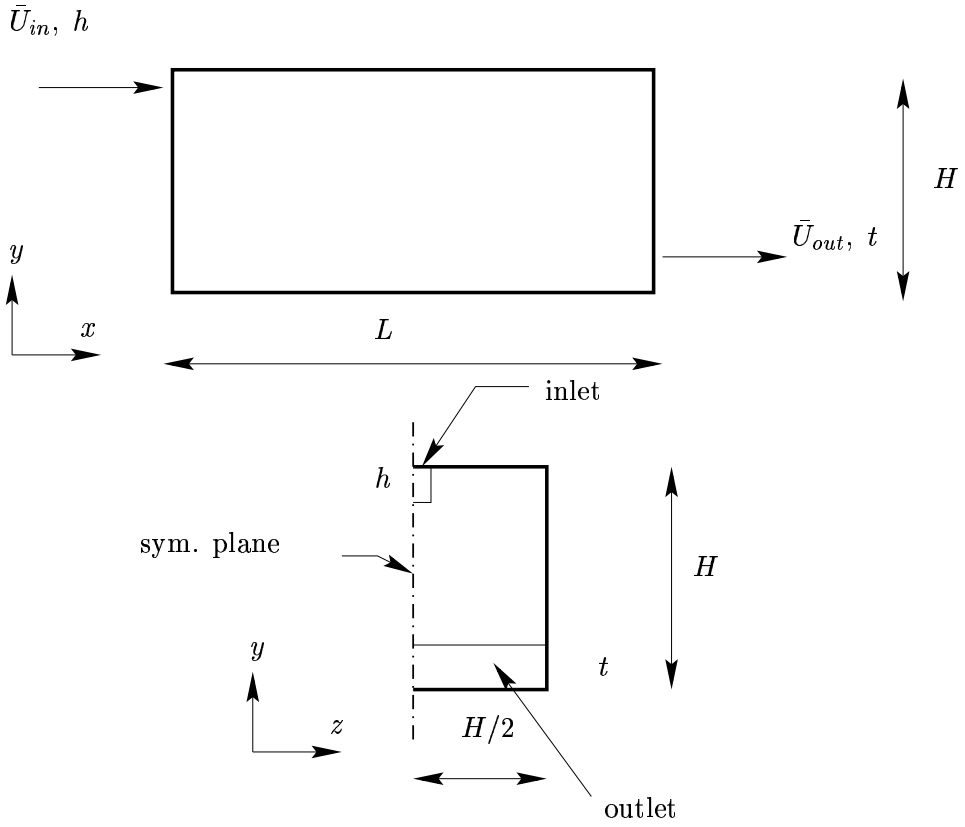

Figure 3: Configuration. $L = 3H$, $h/H = 0.01$, $t/H = 0.15$. $Re = \bar{U}_{in}h/\nu = 7000$.

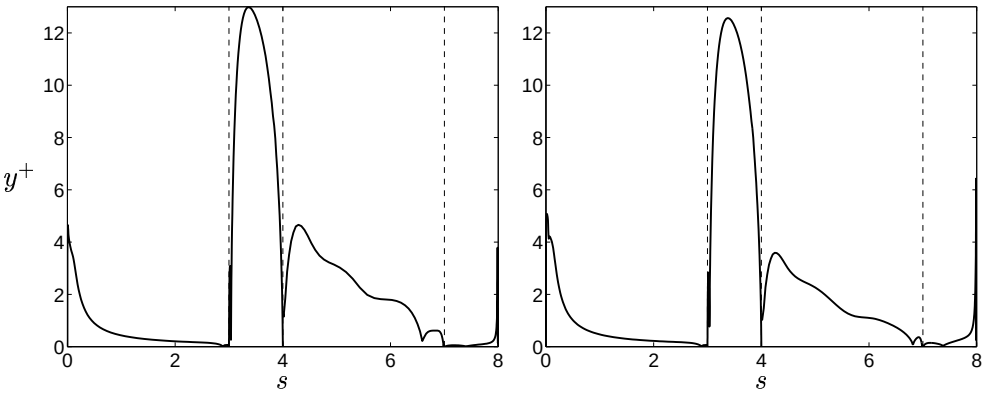

(a) Mesh 1. (b) Mesh 2.

Figure 4: y^+ for the near-wall nodes along the perimeter of the domain. AKN model. $z = 0$. $0 \leq s \leq 3$: wall at $y = H$; $3 \leq s \leq 4$: wall at $x = L$; $4 \leq s \leq 7$: wall at $y = 0$; $7 \leq s \leq 8$: wall at $x = 0$. Dashed lines indicates where the walls start and end.

are shown. It can be seen that the results are fairly grid independent. The spreading rates $d\tilde{y}_{1/2}/dx$ and $dz_{1/2}/dx$ are both close to 0.065. This is in disagreement with experiment from where it is known that the spreading rate in the wall-normal direction (y) is much smaller than the one in the spanwise direction (z). The reason is that the turbulence in the wall-normal direction is dampened by the wall. The experimental values are $d\tilde{y}_{1/2}/dx = 0.065$ and $dz_{1/2}/dx = 0.32$ according to the measurement by Abrahamsson *et al.* (1997).

The predicted spreading $\tilde{y}_{1/2}$ and $z_{1/2}$, contours of $\bar{U}$ and ν_t in Figs. 11-16 using the $\overline{v^2} - f$ model show that the predictions are fairly grid-independent. Comparing $\tilde{y}_{1/2}$ and $z_{1/2}$ with the corresponding predictions with the AKN model in Figs. 5 and 8 it can be seen that, as expected, the predicted spreading of the wall jet is larger with the AKN model than with the $\overline{v^2} - f$ model. The reason is that the wall-normal stress $\overline{v^2}$ in the $\overline{v^2} - f$ model is dampened by the reduced f as the wall is approached. When $\overline{v^2}$ is reduced, so is also the turbulent viscosity and thereby also the entrainment. The reduced entrainment results in higher streamwise velocity, which can be seen by comparing Figs. 12 and 15 with Figs. 6 and 9

In Figs. 17 and 18 the effect of Modification I is investigated. It can be seen from Fig. 17 that without Modification I the predicted $\overline{v^2}$ becomes much larger than $2k/3$, which is physically incorrect. However, with Modification I, $\overline{v^2} \leq 2k/3$ as required. It can be noted that the effect on f is hardly noticeable (cf. Figs. 17c and Figs. 17d). As $\overline{v^2}$ is over-predicted, this also

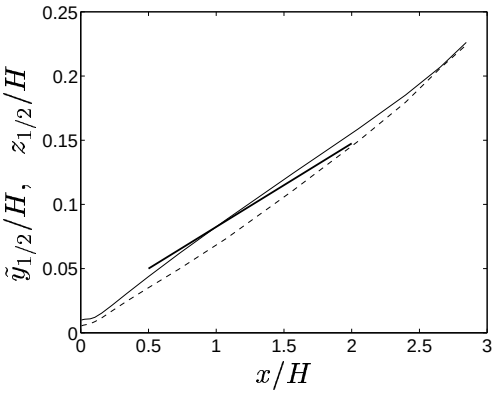

(a) Thin solid line: $\tilde{y}_{1/2}$; dashed line: $z_{1/2}$; thick solid line: $0.065x$.

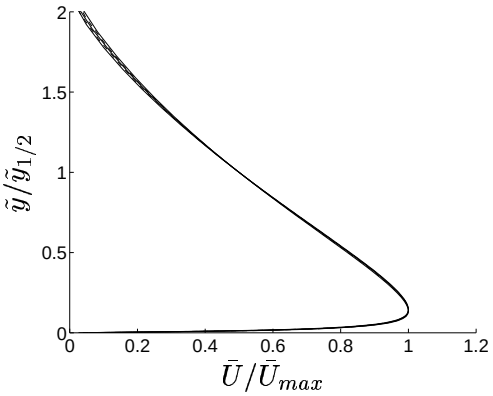

(b) Vertical velocity profile.

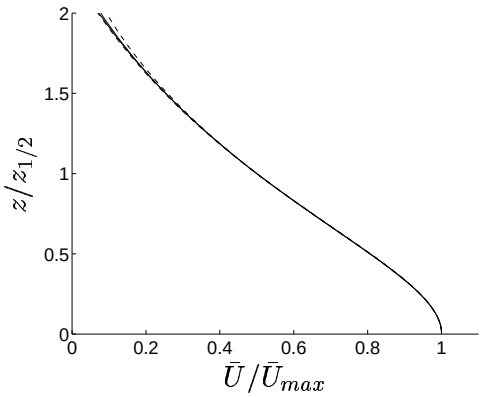

(c) Horizontal velocity profile.

Figure 5: Spreading of the wall jet; vertical and horizontal velocity profiles between $x/H = 0.34$ and $x/H = 1.07$. $\tilde{y} = H - y$. AKN model. Mesh 1.

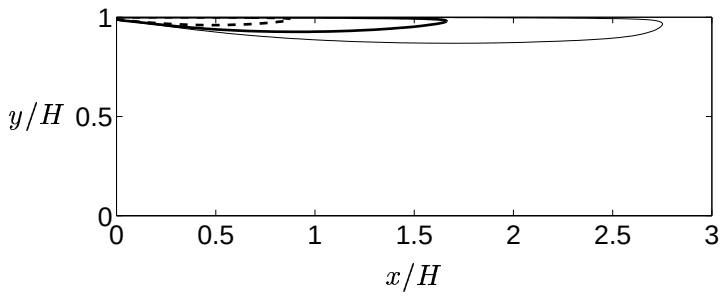

(a) Symmetry plane $z = 0$.

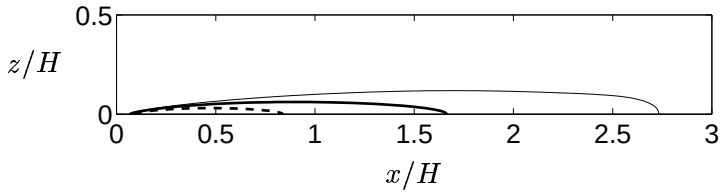

(b) Horizontal plane $y/H = 0.98$.

Figure 6: Contours of $\bar{U}$ velocity. AKN model. Thin solid line: $\bar{U}/\bar{U}_{in} = 0.028$; thick solid line: $\bar{U}/\bar{U}_{in} = 0.056$; thick dashed line: $\bar{U}/\bar{U}_{in} = 0.113$. Mesh 1.

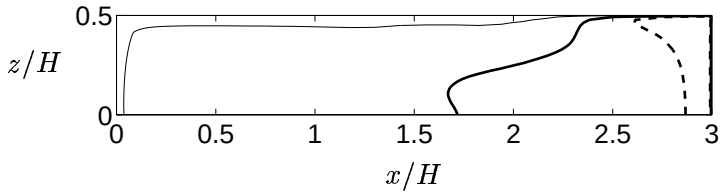

(a) Horizontal plane $y/H = 0.2$.

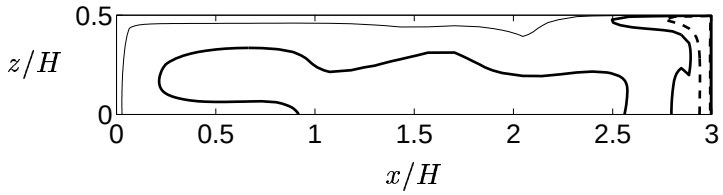

(b) Horizontal plane $y/H = 0.5$.

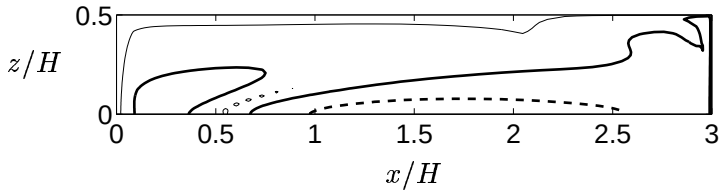

(c) Horizontal plane $y/H = 0.9$.

Figure 7: Contours of turbulent viscosity. AKN model. Thin solid line: $\nu_t/\nu = 10$*; thick solid line:* $\nu_t/\nu = 50$*; thick dashed line:* $\nu_t/\nu = 100$*. Mesh 1.*

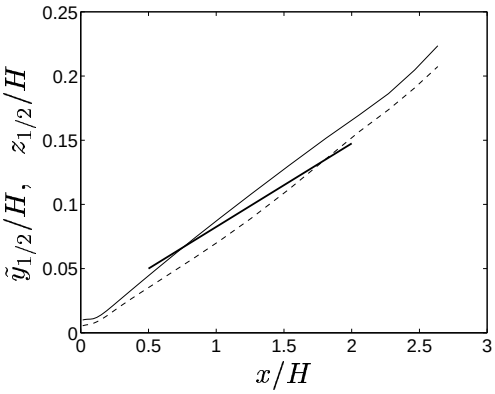

(a) Thin solid line: $\tilde{y}_{1/2}$; dashed line: $z_{1/2}$; thick solid line: $0.065x$.

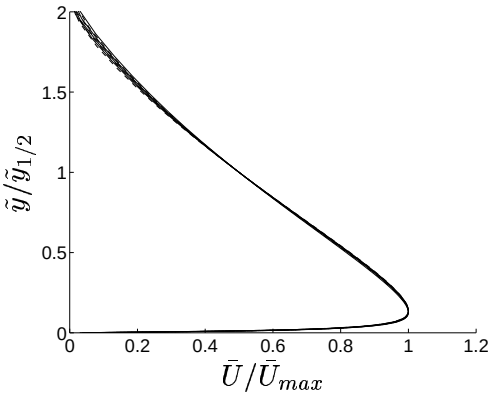

(b) Vertical velocity profile.

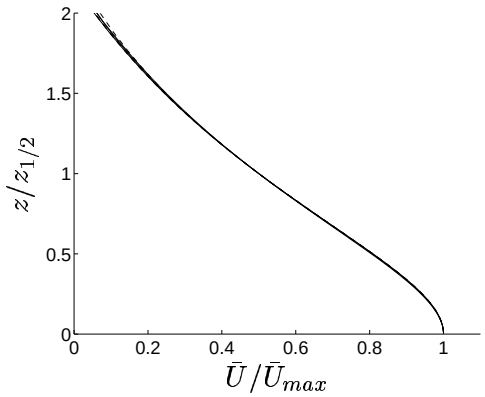

(c) Horizontal velocity profile.

Figure 8: Spreading of the wall jet; vertical and horizontal velocity profiles between $x/H = 0.3$ and $x/H = 1.8$. $\tilde{y} = H - y$. AKN model. Mesh 2.

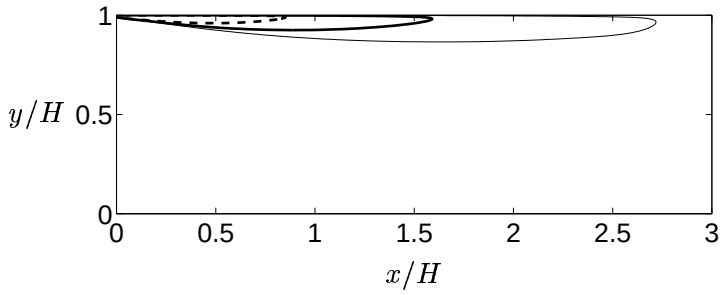

(a) Symmetry plane $z = 0$.

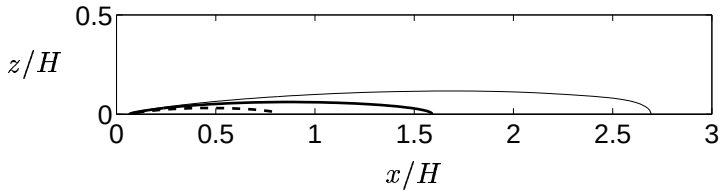

(b) Horizontal plane $y/H = 0.98$.

Figure 9: Contours of $\bar{U}$ velocity. AKN model. Thin solid line: $\bar{U}/\bar{U}_{in} = 0.028$; thick solid line: $\bar{U}/\bar{U}_{in} = 0.056$; thick dashed line: $\bar{U}/\bar{U}_{in} = 0.113$. Mesh 2.

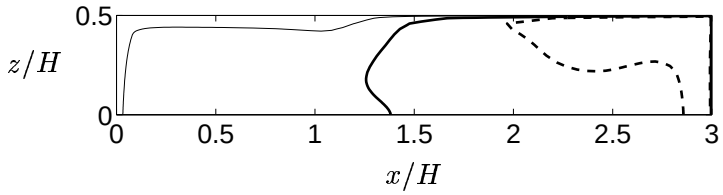

(a) Horizontal plane $y/H = 0.2$.

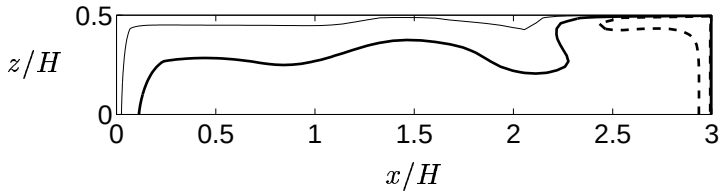

(b) Horizontal plane $y/H = 0.5$.

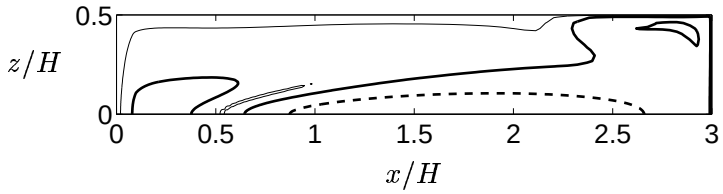

(c) Horizontal plane $y/H = 0.9$.

Figure 10: Contours of turbulent viscosity. AKN model. Thin solid line: $\nu_t/\nu = 10$*; thick solid line:* $\nu_t/\nu = 50$*; thick dashed line:* $\nu_t/\nu = 100$*. Mesh 2.*

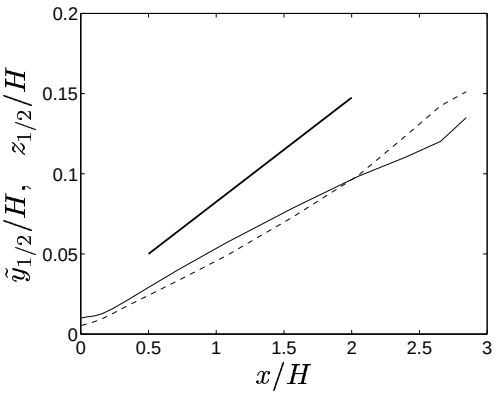

(a) Thin solid line: $\tilde{y}_{1/2}$; dashed line: $z_{1/2}$; thick solid line: $0.065x$.

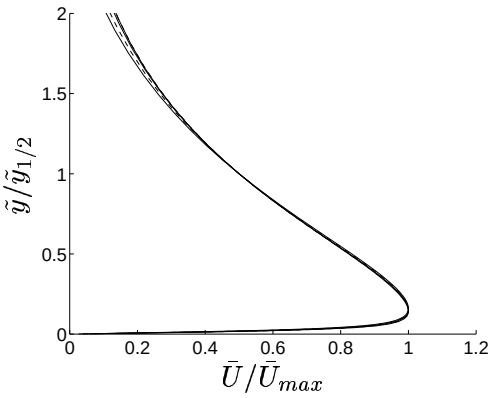

(b) Vertical velocity profile.

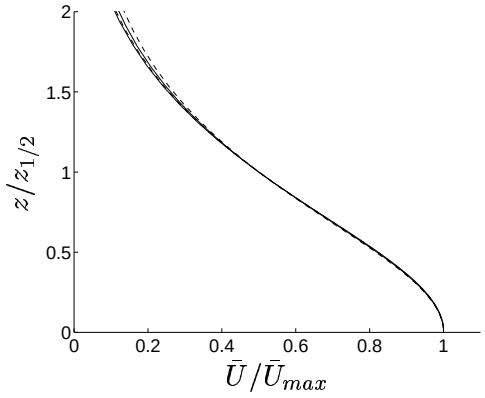

(c) Horizontal velocity profile.

Figure 11: Spreading of the wall jet; vertical and horizontal velocity profiles between $x/H = 0.3$ and $x/H = 1.8$. $\tilde{y} = H - y$. $\overline{v^2} - f$ model, Modification I. Mesh 1.

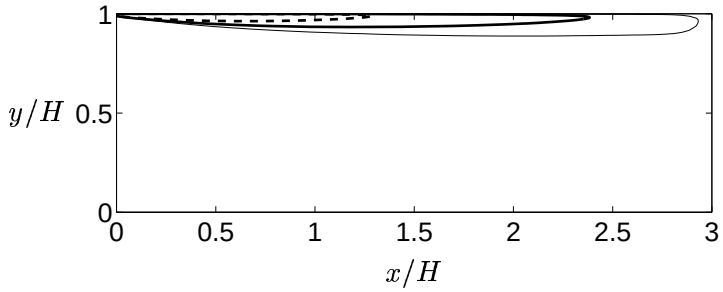

(a) Symmetry plane $z = 0$.

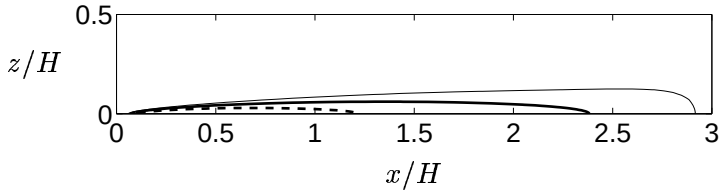

(b) Horizontal plane $y/H = 0.98$.

Figure 12: Contours of $\bar{U}$ velocity. $\overline{v^2} - f$ model, Modification I. Thin solid line: $\bar{U}/\bar{U}_{in} = 0.028$; thick solid line: $\bar{U}/\bar{U}_{in} = 0.056$; thick dashed line: $\bar{U}/\bar{U}_{in} = 0.113$. Mesh 1.

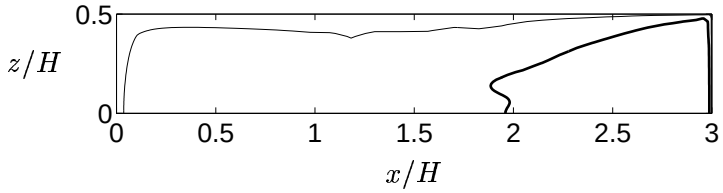

(a) Horizontal plane $y/H = 0.2$.

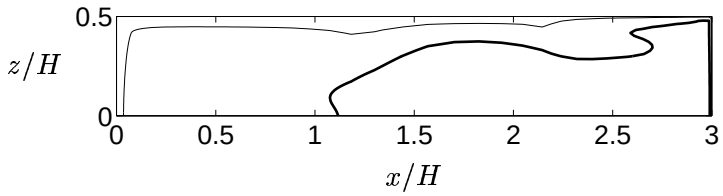

(b) Horizontal plane $y/H = 0.5$.

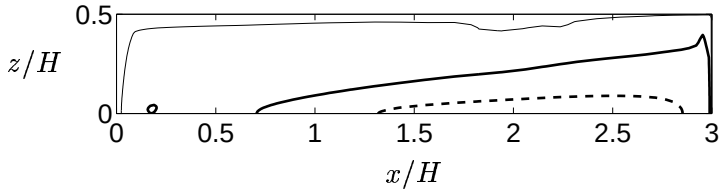

(c) Horizontal plane $y/H = 0.9$.

Figure 13: Contours of turbulent viscosity. $\overline{v^2} - f$ model, Modification I. Thin solid line: $\nu_t/\nu = 10$; thick solid line: $\nu_t/\nu = 50$; thick dashed line: $\nu_t/\nu = 100$. Mesh 1

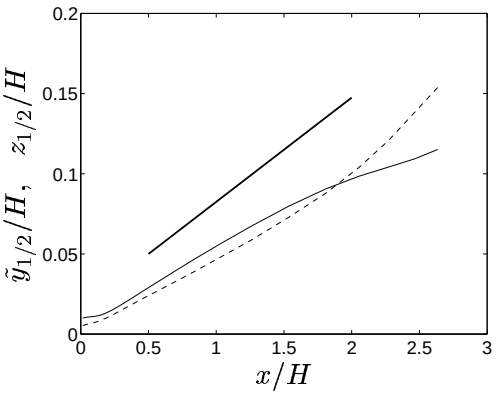

(a) Thin solid line: $\tilde{y}_{1/2}$; dashed line: $z_{1/2}$; thick solid line: $0.065x$.

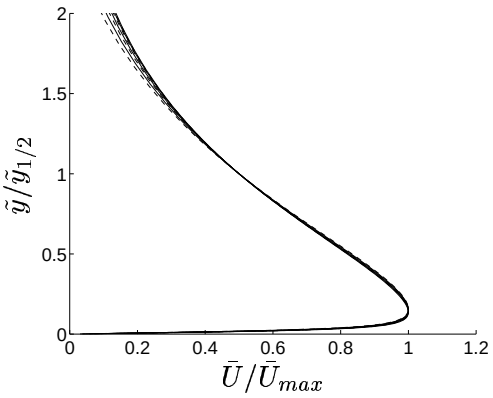

(b) Vertical velocity profile.

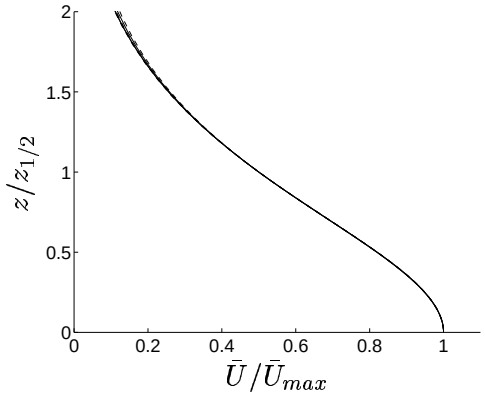

(c) Horizontal velocity profile.

Figure 14: Spreading of the wall jet; vertical and horizontal velocity profiles between $x/H = 0.3$ and $x/H = 1.8$. $\tilde{y} = H - y$. $\overline{v^2} - f$ model, Modification I. Mesh 2.

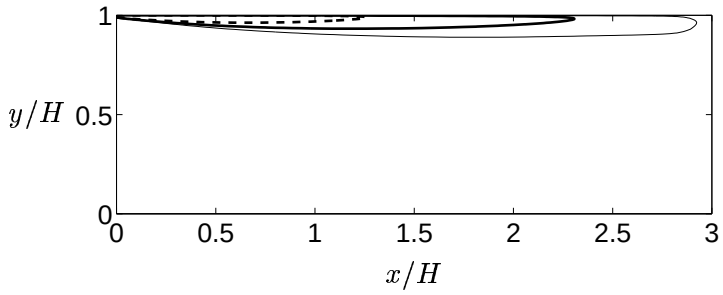

(a) Symmetry plane $z = 0$.

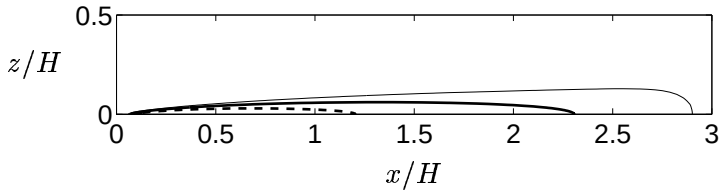

(b) Horizontal plane $y/H = 0.98$.

Figure 15: Contours of $\bar{U}$ velocity. $\overline{v^2} - f$ model. Thin solid line: $\bar{U}/\bar{U}_{in} = 0.028$; thick solid line: $\bar{U}/\bar{U}_{in} = 0.056$; thick dashed line: $\bar{U}/\bar{U}_{in} = 0.113$. Mesh 2.

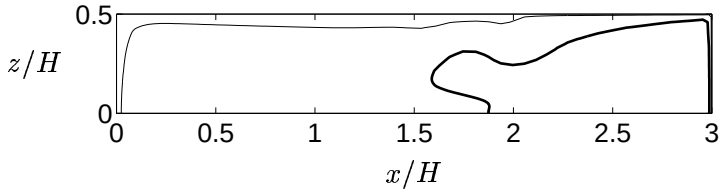

(a) Horizontal plane $y/H = 0.2$.

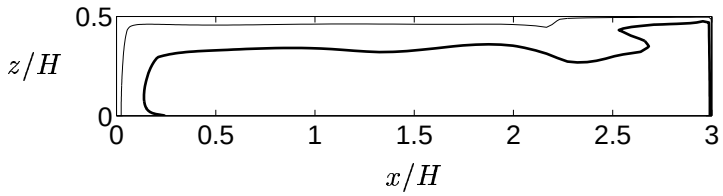

(b) Horizontal plane $y/H = 0.5$.

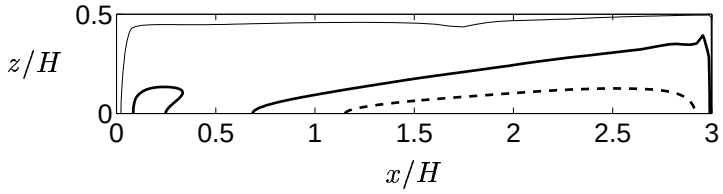

(c) Horizontal plane $y/H = 0.9$.

Figure 16: Contours of turbulent viscosity. $\overline{v^2} - f$ model, Modification I. Thin solid line: $\nu_t/\nu = 10$; thick solid line: $\nu_t/\nu = 50$; thick dashed line: $\nu_t/\nu = 100$. Mesh 2.

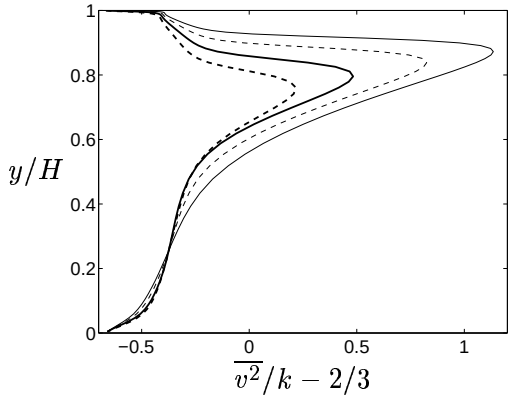

(a) Standard $\overline{v^2} - f$ model.

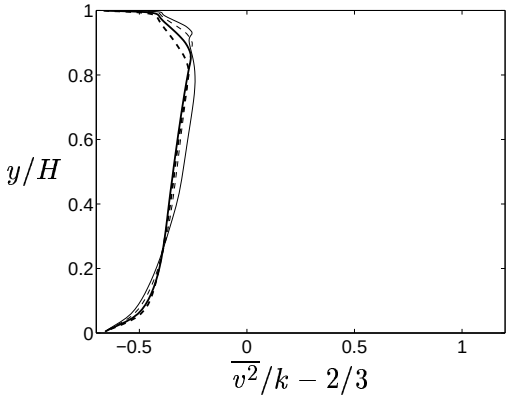

(b) $\overline{v^2} - f$ model, Modification I.

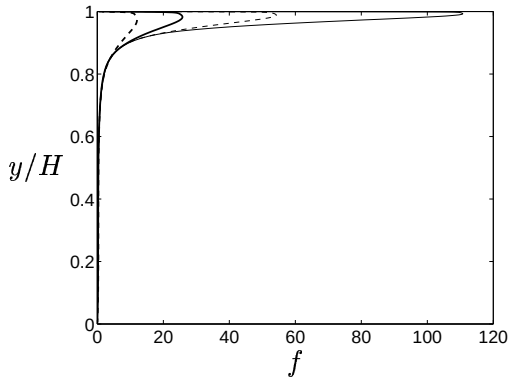

(c) Standard $\overline{v^2} - f$ model.

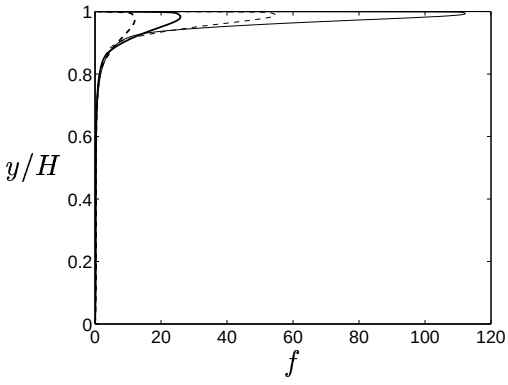

(d) $\overline{v^2} - f$ model, Modification I.

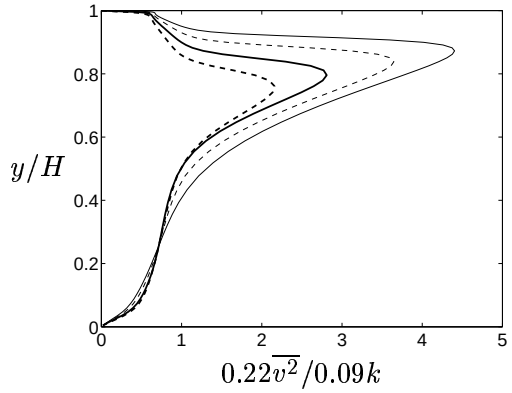

(e) Standard $\overline{v^2} - f$ model.

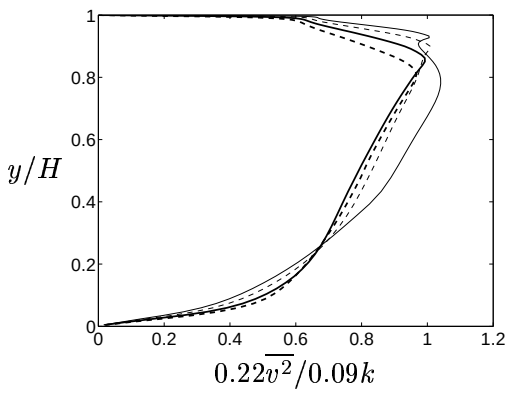

(f) $\overline{v^2} - f$ model, Modification I.

Figure 17: Profiles of $(\overline{v^2}/k - 2/3)$ *and* f *between* $x/H = 0.34$ *and* $x/H = 1.07$. *Thin solid line:* $x/H = 0.34$*; thick dashed line:* $x/H = 1.07$. *Comparison between standard* $\overline{v^2} - f$ *model and Modification I. Mesh 1.*

gives an over-predicted turbulent viscosity compared with a $k-\varepsilon$ model. The ratio of these two viscosities, $0.22\overline{v^2}/(0.09k)$ (See Eq. 19), is shown in Fig. 17e and f. As can be seen, ν_t is over-predicted with up to a factor of four in the outer shear layer of the wall jet compared with a $k-\varepsilon$ model. Please recall that in Modification I ν_t is computed from Eq. 19.

In Craft & Launder (2001) it was shown that the reason why the spreading rate in the lateral (z) direction is much larger than that in the wall-normal direction (y) is due to a strong secondary motion in the $y-z$ plane, driven by the anisotropy in the normal stresses. Thus a Reynolds stress model is required to predict this flow in a proper way. One way to create anisotropic normal stresses in an eddy-viscosity model is to use anisotropic turbulent viscosities.

Below results using the $\overline{v^2}-f$ model with anisotropic turbulent viscosities are presented. In Figs. 19-21 the predicted thickness of the wall jet, velocity profiles and profiles are depicted for Modification I and II. In Modification II different viscosities are used for the diffusion terms in the wall-normal direction ($\nu_{t,\perp}$) and in the wall-parallel direction ($\nu_{t,\parallel}$). The viscosity in the wall-normal direction is taken from the $\overline{v^2}-f$ model and the viscosity in the wall-parallel direction is computed with the $k-\varepsilon$ expression. The ratio between these viscosities is $\nu_{t,\perp}/\nu_{t,\parallel}=0.22\overline{v^2}/(0.09k)$, see Eq. 20. The expected effect is that the spreading of the wall jet in the spanwise direction with this modification should be larger than with Modification I. Comparing Figs. 19 and 14 we find that this is indeed the case. Actually the spreading in the wall-normal direction has also increased somewhat, but clearly $z_{1/2}/\tilde{y}_{1/2}$ is larger in Fig. 19 than in Fig. 14. Also by comparing the isoline of $\bar{U}$ in Figs. 20 and 15 it can be seen that the spreading with Modification I+II is larger than with Modification I.

The ratio $\nu_{t,\perp}/\nu_{t,\parallel}$ is shown in Fig. 21, both as profiles and as contours of isolines. It can be seen that $\nu_{t,\perp}$ is much smaller than $\nu_{t,\parallel}$. The ratio $\nu_{t,\perp}/\nu_{t,\parallel}$ is approximately 0.6 at the location of the velocity peak ($\tilde{y}/\tilde{y}_{1/2}\simeq 0.15$, see Fig. 19a). Inside the velocity peak the ratio goes to zero as $\overline{v^2}$ is dampened by wall ($f\rightarrow 0$).

6 Conclusions

Two modifications of the $\overline{v^2}-f$ model have been presented. In the first modification – Modification I – the source term in the $\overline{v^2}$ equation is limited so as to ensure that $\overline{v^2}<2k/3$. The second modification – Modification II – is based on a non-isotropic eddy-viscosity approach. Different viscosities are used for the turbulent diffusion in the wall-normal direction and in the wall-parallel direction. The object of Modification II was to be able to model the different spreading rates in the wall-normal and spanwise direction of a 3D wall jet.

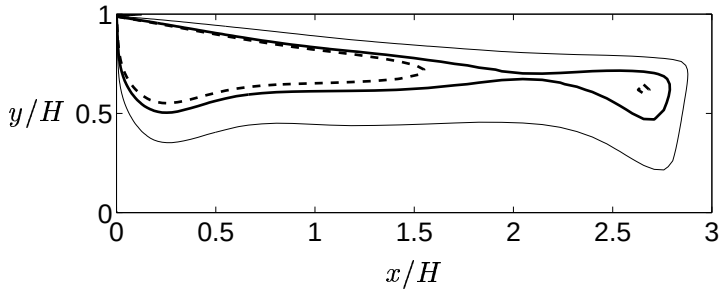

(a) Standard $\overline{v^2} - f$ model. $y/H = 0.98$

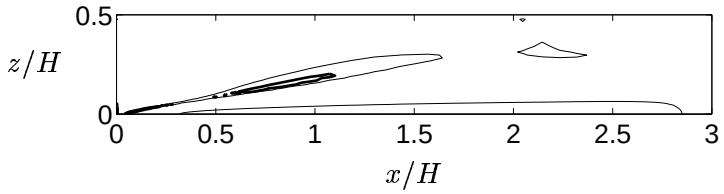

(b) Standard $\overline{v^2} - f$ model. $z = 0$

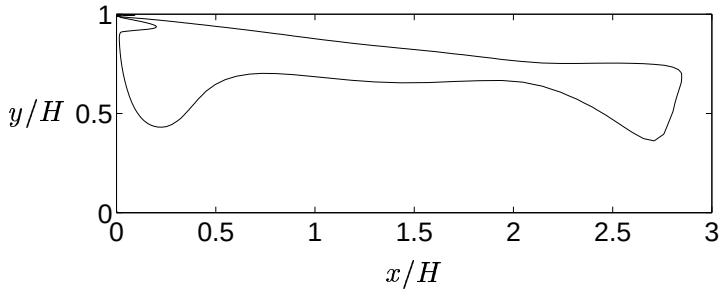

(c) $\overline{v^2} - f$ model, Modification I. $y/H = 0.98$

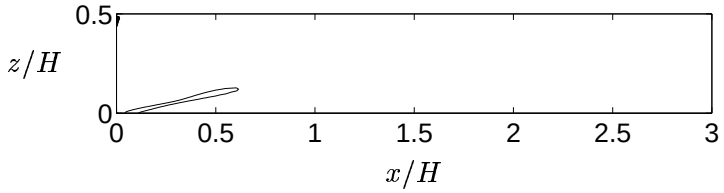

(d) $\overline{v^2} - f$ model, Modification I. $z = 0$

Figure 18: Contour lines of $\overline{v^2}/k - 2/3$. *Thin solid lines:* $\overline{v^2}/k - 2/3 = -0.3$; *thick solid lines:* $\overline{v^2}/k - 2/3 = -0.1$; *thin dashed lines:* $\overline{v^2}/k - 2/3 = 0$. *Comparison between standard* $\overline{v^2} - f$ *model and modified* $\overline{v^2} - f$ *model in which source term in* $\overline{v^2}$ *equation was limited. Mesh 1.*

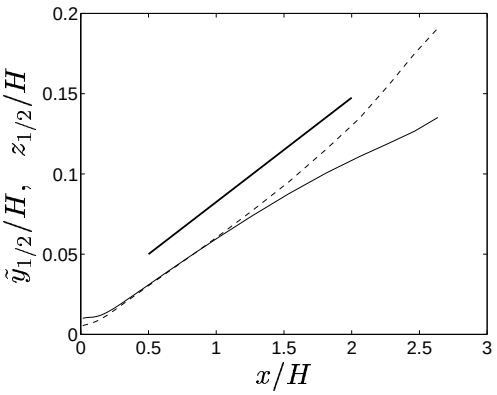

(a) Thin solid line: $\tilde{y}_{1/2}$; dashed line: $z_{1/2}$; thick solid line: $0.065x$.

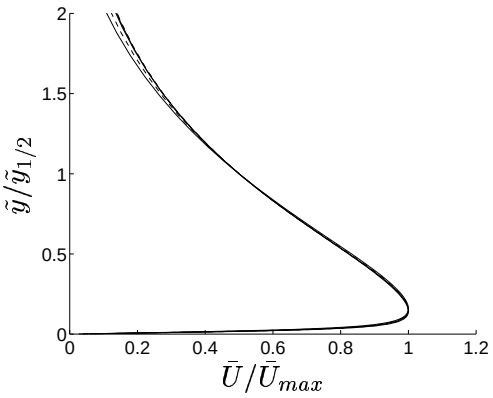

(b) Vertical velocity profile.

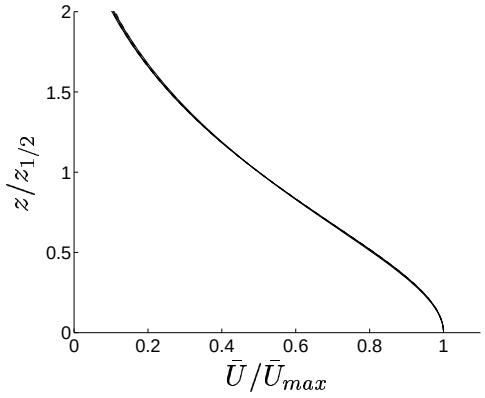

(c) Horizontal velocity profile.

Figure 19: Spreading of the wall jet; vertical and horizontal velocity profiles between $x/H = 0.3$ and $x/H = 1.8$. $\tilde{y} = H - y$. $\overline{v^2} - f$ model, Modification I and II. Mesh 2.

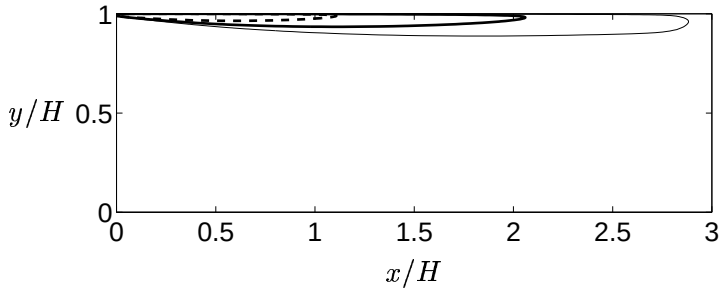

(a) Symmetry plane $z = 0$.

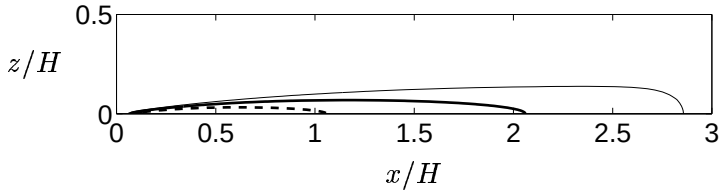

(b) Horizontal plane $y/H = 0.98$.

Figure 20: Contours of $\bar{U}$ velocity. $\overline{v^2} - f$ model, Modification I and II. Thin solid line: $\bar{U}/\bar{U}_{in} = 0.028$; thick solid line: $\bar{U}/\bar{U}_{in} = 0.056$; thick dashed line: $\bar{U}/\bar{U}_{in} = 0.113$. Mesh 2.

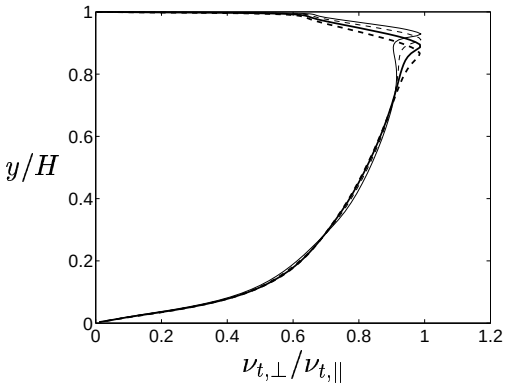

(a) Profiles between $x/H = 0.34$ and $x/H = 1.07$.

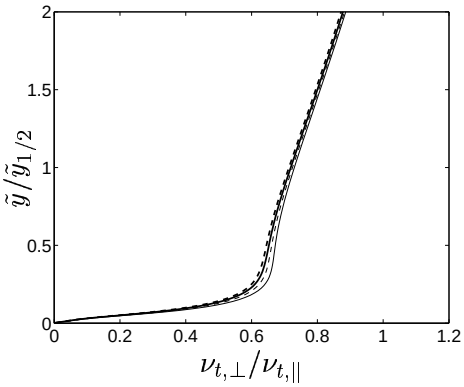

(b) Profiles between $x/H = 0.34$ and $x/H = 1.07$. $\tilde{y} = H - y$.

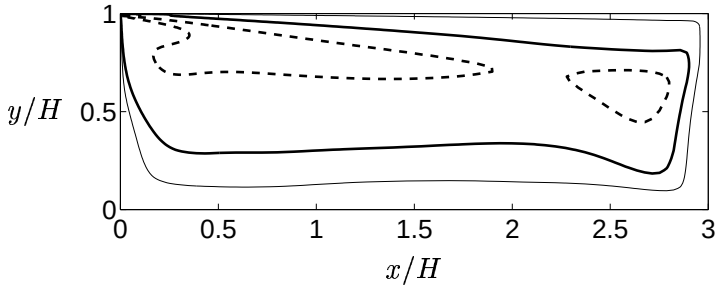

(c) Isolines of $\nu_{t,\perp}/\nu_{t,||}$. $y/H = 0.98$. Thin solid lines: 0.5; thick solid lines: 0.7; thin dashed lines: 0.9.

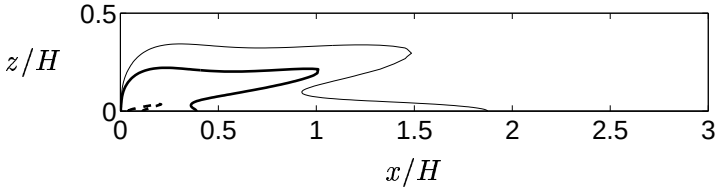

(d) Isolines of $\nu_{t,\perp}/\nu_{t,||}$. Thin solid lines: 0.5; thick solid lines: 0.7; thin dashed lines: 0.9.

Figure 21: $\overline{v^2} - f$ model, Modification I and II. Mesh 2. $\nu_{t,\perp}/\nu_{t,||}$

Modification I was shown to work well. The predicted $\overline{v^2}$ was smaller than $2k/3$ both for the fully developed channel flow and the 3D wall jet. Modification II was found to give only a small improvement for the 3D wall jet, and with this modification the spanwise spreading rate was increased.

References

ABE, K., KONDOH, T. & NAGANO, Y. 1994 A new turbulence model for predicting fluid flow and heat transfer in separating and reattaching flows - 1. Flow field calculations. *Int. J. Heat Mass Transfer* **37**, 139–151.

ABRAHAMSSON, H., JOHANSSON, B. & LÖFDAHL, L. 1997 The turbulence field of a fully developed three-dimensional wall jet. Report 97/1. Dept. of Thermo and Fluid Dynamics, Chalmers University of Technology, Gothenburg.

CRAFT, T. & LAUNDER, B. 2001 On the spreading mechanism of the three-dimensional turbulent wall jet. *Journal of Fluid Mechanics* **435**, 305–326.

DAVIDSON, L. 1995 Prediction of the flow around an airfoil using a Reynolds stress transport model. *ASME: Journal of Fluids Engineering* **117**, 50–57.

DAVIDSON, L. 2002 MTF270 turbulence modelling. Lecture notes, www.tfd.chalmers.se/doct/comp_turb_model/, Dept. of Thermo and Fluid Dynamics, Chalmers University of Technology, Göteborg, Sweden.

DAVIDSON, L. & FARHANIEH, B. 1995 CALC-BFC: A finite-volume code employing collocated variable arrangement and cartesian velocity components for computation of fluid flow and heat transfer in complex three-dimensional geometries. Rept. 95/11. Dept. of Thermo and Fluid Dynamics, Chalmers University of Technology, Gothenburg.

DURBIN, P. 1991 Near-wall turbulence closure modeling without damping functions. *Theoretical and Computational Fluid Dynamics* **3**, 1–13.

DURBIN, P. 1993 Application of a near-wall turbulence model to boundary layers and heat transfer. *International Journal of Heat and Fluid Flow* **14** (4), 316–323.

DURBIN, P. 1996 On the $k-3$ stagnation point anomaly. *International Journal of Heat and Fluid Flow* **17**, 89–90.

LAUNDER, B., REECE, G. & RODI, W. 1975 Progress in the development of a Reynolds-stress turbulence closure. *Journal of Fluid Mechanics* **68** (3), 537–566.

VAN LEER, B. 1974 Towards the ultimate conservative difference scheme. Monotonicity and conservation combined in a second order scheme. *Journal of Computational Physics* **14**, 361–370.

LIEN, F.-S. & KALITZIN, G. 2001 Computations of transonic flow with the v2f turbulence model. *International Journal of Heat and Fluid Flow* **22** (1), 53–61.

MOSER, R., KIM, J. & MANSOUR, N. 1999 Direct numerical simulation of turbulent channel flow up to $Re_\tau = 590$. *Physics of Fluids A* **11**, 943–945.

PALLARES, J. & DAVIDSON, L. 2000 Large-eddy simulations of turbulent flows in stationary and rotating channels and in a stationary square duct. Report 00/03. Dept. of Thermo and Fluid Dynamics, Chalmers University of Technology.

PATANKAR, S. 1980 *Numerical Heat Transfer and Fluid Flow*. New York: McGraw-Hill.